ACCELERATED COMMUNICATION

Neutralizing antibodies targeting the SARS-CoV-2 receptor binding domain isolated from a naïve human antibody library

Benjamin N. Bell[1,2] | Abigail E. Powell[2,3] | Carlos Rodriguez[4] | Jennifer R. Cochran[5,6] | Peter S. Kim[2,3,7]

[1]Department of Molecular and Cellular Physiology, Stanford University School of Medicine, Stanford, California

[2]Stanford ChEM-H, Stanford University, Stanford, California

[3]Department of Biochemistry, Stanford University School of Medicine, Stanford, California

[4]xCella Biosciences, Menlo Park, California

[5]Department of Bioengineering, Stanford University, Stanford, California

[6]Department of Chemical Engineering, Stanford University, Stanford, California

[7]Chan Zuckerberg Biohub, San Francisco, California

Correspondence
Peter S. Kim, Stanford ChEM-H/Neuro Building, W220, Stanford University, 290 Jane Stanford Way, Stanford, CA 94305, USA.
Email: kimpeter@stanford.edu

Present address
Carlos Rodriguez, Stanford Innovative Medicines Accelerator, Stanford, California

Funding information
Chan Zuckerberg Biohub; Frank Quattrone and Denise Foderaro Family Research Fund; National Science Foundation, Grant/Award Number: Graduate Research Fellowship; Stanford Maternal and Child Health Research Institute, Grant/Award Number: Postdoctoral Fellowship; Virginia and D. K. Ludwig Fund for Cancer Research

Abstract

Infection with SARS-CoV-2 elicits robust antibody responses in some patients, with a majority of the response directed at the receptor binding domain (RBD) of the spike surface glycoprotein. Remarkably, many patient-derived antibodies that potently inhibit viral infection harbor few to no mutations from the germline, suggesting that naïve antibody libraries are a viable means for discovery of novel SARS-CoV-2 neutralizing antibodies. Here, we used a yeast surface-display library of human naïve antibodies to isolate and characterize three novel neutralizing antibodies that target the RBD: one that blocks interaction with angiotensin-converting enzyme 2 (ACE2), the human receptor for SARS-CoV-2, and two that target other epitopes on the RBD. These three antibodies neutralized SARS-CoV-2 spike-pseudotyped lentivirus with IC$_{50}$ values as low as 60 ng/ml in vitro. Using a biolayer interferometry-based binding competition assay, we determined that these antibodies have distinct but overlapping epitopes with antibodies elicited during natural COVID-19 infection. Taken together, these analyses highlight how in vitro selection of naïve antibodies can mimic the humoral response in vivo, yielding neutralizing antibodies and various epitopes that can be effectively targeted on the SARS-CoV-2 RBD.

KEYWORDS

COVID-19, neutralizing antibody, RBD, SARS-CoV-2, yeast surface display

1 | INTRODUCTION

Over 100 million cases of Coronavirus Disease 2019 (COVID-19) and 2.3 million deaths worldwide in the past 12 months[1] have been caused by the novel human pathogen SARS-CoV-2.[2,3] Since the beginning of the COVID-19 pandemic, extensive work has been devoted to characterizing the antibody response to SARS-CoV-2 in response to both infection[4–13] and vaccination.[14–20] Analysis of antibody responses has revealed that patients elicit robust neutralizing antibodies targeting the SARS-CoV-2 spike,[6–8,12,21] a trimeric glycoprotein responsible for receptor recognition and host cell entry.[2,22,23] Specifically, the spike receptor binding domain (RBD), which binds the host cell receptor ACE2, has been shown to be an immunodominant region of the spike.[6–9,12] Despite being only 25 kDa in size, the RBD elicits antibodies that fall into several subclasses targeting distinct, but overlapping, epitopes.[7,10] Many of these subclasses contain neutralizing antibodies, demonstrating that multiple sites on the RBD are vulnerable to inhibition and raising the possibility that RBD-targeting antibodies neutralize viral entry via a variety of mechanisms of action.

Remarkably, many RBD antibodies described to date have high similarity to their germline antibody precursors, with low rates of somatic hypermutation.[6–8,10] This observation is encouraging for RBD- and spike-based vaccine approaches, as it suggests that neutralizing antibodies can readily be elicited in healthy individuals. This germline similarity also highlights the potential use of naïve antibody libraries as a promising source of novel therapeutic antibodies and for comparison of clones selected in vitro to those elicited by natural COVID-19 infection or vaccination.

In order to identify RBD-targeting antibodies with high similarity to the germline, here we employed an in vitro approach based on a yeast surface-display library of human naïve antibodies expressed in a single-chain variable fragment (scFv) format. We subsequently isolated and characterized three novel neutralizing antibodies: one (ABP18) that blocks binding of RBD to ACE2, and two (NBP10, NBP11) that do not. These three antibodies neutralize SARS-CoV-2 spike-pseudotyped lentivirus in vitro with IC_{50} (half-maximal inhibitory concentration) values of 0.06–13 μg/ml. When we performed binding competition experiments using biolayer interferometry (BLI), we found that ABP18, NBP10, and NBP11 have epitopes that are distinct but overlap with epitopes that are well-defined of antibodies elicited by natural COVID-19 infection. Taken together, these analyses demonstrate that in vitro selections of naïve antibodies can mimic the humoral response in vivo to identify neutralizing antibodies. In vitro selections therefore may constitute an important tool for both vaccine development and antibody discovery for SARS-CoV-2 therapeutics.

2 | MATERIALS AND METHODS

2.1 | Yeast surface display selections

xEmplar™ is a proprietary naïve antibody library developed by xCella Biosciences that incorporates a selection of antibody scaffolds (VH, VL, JL, JH) to reflect the relative abundance and diversity of antibody germlines in humans.[24] The D segments of this library were modified to enhance developability via the elimination of certain motifs. The library was synthesized in a single-chain variable fragment (scFv) format and transformed into *Saccharomyces cerevisiae*, resulting in a surface-display library with estimated diversity of ∼1×10^9.

A total of five rounds of sorting were conducted to isolate scFv-displaying yeast that could bind the SARS-CoV-2 spike RBD and disrupt ACE2/RBD interactions. The antigens used for the selections were His-tagged RBD from Ray Biotech (Cat. # 230–30,162), His-tagged and Avi-Tagged RBD from ACROBiosystems (Cat. # SPD-C82E9), and His-tagged and Avi-Tagged ACE2 from ACROBiosystems (Cat. # AC2-H82E6). Two initial rounds of magnetic-activated cell sorting were performed on the library using decreasing amounts of Ray Biotech RBD-coated His-Tag Dynabeads (Thermo Fisher). The resulting enriched library pool was subsequently sorted using a Sony SH800 Cell Sorter. Round 3 selected for variants that bound 200 nM RBD (Ray Biotech). Round 4 enriched for variants that bound 100 nM RBD (ACROBiosystems). In Round 5, the ACE2/RBD blocking sort, the enriched library was incubated with 100 nM RBD (Ray Biotech) for 1 h at room temperature, washed once using phosphate-buffered saline (pH 7.4) with 0.1% bovine serum albumin (PBSA), then incubated with secondary antibody for 15 min on ice to detect RBD binding. The resulting complex was washed twice with PBSA, incubated with 100 nM ACE2 (ACROBiosystems) for 30 min on ice, and washed once more with PBSA. Last, the cells were incubated with 1:1000 dilution of Streptavidin-Alexa Fluor 647 (Thermo Fisher Scientific Cat. # S32357) on ice for 15 min for detection of ACE2 binding.

Yeast scFv display levels were evaluated prior to sorting (data not shown) by incubating the yeast with a 1:1000 dilution of Chicken anti C-MYC Epitope Tag Primary Antibody from Exalpha Biologicals Inc. (Catalog No. ACMYC), followed by incubation with a 1:1000 dilution of Goat anti-Chicken IgY (H + L) Cross Adsorbed Secondary Antibody, Alexa Fluor Plus 647 from Thermo Fisher Scientific (Catalog No. A32933).

RBD antigen binding during selection rounds 3 and 5 was evaluated using a 1:1000 dilution of rabbit anti-His FITC secondary antibody (Bethyl Laboratories). RBD antigen binding during selection Round 4 was evaluated using a 1:1000 dilution of Streptavidin-Alexa Fluor 647 secondary (Jackson ImmunoResearch). Use of a different secondary reagent selected for true RBD binders and de-enriched the population for anti-His-tag secondary reagent binders (data not shown). In subsequent selections, such secondary reagent binders would give the false impression of being ACE2-blocking antibodies.

After Round 5, plasmid DNA was isolated from the sorted yeast populations using a Zymoprep Yeast Miniprep II Kit (Zymo Research). Stellar cells (Takara) were transformed with these polyclonal plasmid DNA mixtures and streaked to single colonies on LB agar plates supplemented with 100 μg/ml carbenicillin. Single-colony cultures were propagated in 2xYT medium supplemented with 100 μg/ml carbenicillin and the sequences of mini-prepped plasmids were analyzed to identify scFvs ABP18, NBP10, NBP11, and NBP18.

2.2 | Plasmid cloning and propagation

Variable heavy chain and variable light chain were PCR-amplified from yeast plasmid DNA and cloned into CMV/R expression vectors encoding human IgG1 constant domains using InFusion (Takara). Similarly, scFv sequences were cloned into a CMV/R expression vector with a C-terminal hexahistidine tag. Plasmid DNA for mammalian expression of the His-tagged SARS-CoV-2 RBD in a pCAGGS vector was kindly provided by Dr. Florian Krammer.[25] Plasmid DNA for expression of His-tagged SARS1 and MERS RBDs under control of a CMV promoter was a kind gift from Dr. John Pak. Plasmid DNA for expression of ACE2-huFc-Avi was previously described.[20] All plasmids were sequence confirmed via Sanger sequencing prior to mammalian transfection.

Plasmids were propagated overnight at 37°C in Stellar cells (Takara) in 2×YT medium supplemented with 100 μg/mL carbenicillin (RBD and ACE2 plasmids) or 50 μg/ml kanamycin (IgG plasmids). Plasmids were isolated using a Machery Nagel maxi prep kit and filtered in a biosafety cabinet using a 0.22 μm filter prior to transfection.

2.3 | Recombinant protein expression and purification

IgGs, scFvs, ACE2-huFc-Avi, and coronavirus RBDs were expressed and purified from Expi293F cells cultured in 33% Expi293 Expression/66% FreeStyle Expression medium (Thermo Fisher Scientific) and grown in baffled polycarbonate shaking flasks (Triforest) at 37°C and 8% CO_2. Cells were grown to a density of $\sim3 \times 10^6$/ml and transiently transfected using FectoPro transfection reagent (Polyplus). Briefly, 0.5 μg DNA per ml final transfection volume was added to culture medium (1/10 volume of final transfection) followed by FectoPro at a concentration of 1.3 μl per ml final transfection volume and incubated at room temperature for 10 min. Transfection mixtures were added to cells, which were then supplemented with D-glucose (4 g/L final concentration) and 2-propylpentanoic (valproic) acid (3 mM final concentration). Cells were harvested 3–5 days after transfection via centrifugation at 18,000g for 15 min. Cell culture supernatants were filtered using a 0.22 μm filter prior to purification.

Filtered Expi cell culture supernatants from ABP18, NBP10, and NBP11 scFv expressions were buffered with 1/10 volume 10× PBS and loaded at a flow rate of 5 ml/min onto a HisTrap excel column (Cytiva) equilibrated in PBS (pH 7.4) on a GE ÄKTA Pure system. The column was subsequently equilibrated with 5 column volumes PBS + 10 mM imidazole (pH 7.4) before elution with 10 column volumes PBS + 250 mM imidazole (pH 7.4). Elutions were concentrated using Amicon spin filters (MWCO 10 kDa; Millipore Sigma) and scFvs were subsequently loaded onto a GE Superdex S200 increase 10/300 GL column pre-equilibrated in PBS (pH 7.4) on a GE ÄKTA Pure system. Protein-containing fractions were identified by A280 signal and/or SDS-PAGE, pooled, and stored at 4°C until use.

Filtered Expi cell culture supernatants from ABP18, NBP10, and NBP11 IgG expressions were buffered with 1× PBS (pH 7.4) and purified using Protein A resin (Pierce). Supernatants were incubated with Protein A resin in batch and then resin/supernatant mixtures were added to glass chromatography columns. Resin was washed with ~10 column volumes of 1× PBS and IgGs were eluted with 100 mM glycine (pH 2.8) and immediately quenched with 1/10 volume 1 M Tris (pH 8.0). ACE2 expressed with a C-terminal human IgG1 Fc and Avi tag was purified in the same way as IgGs.

Antibodies in the competition panel (see BLI [Section 2.7]) were purified on a HiTrap MabSelect SuRe column (Cytiva) equilibrated in PBS (pH 7.4) on a GE ÄKTA Pure system. Filtered Expi cell culture supernatants were buffered with 1/10 volume 10× PBS and loaded at a flow rate of 3.5 ml/min. The column was subsequently equilibrated with 5 column volumes PBS (pH 7.4) before elution with 3 column volumes 100 mM glycine (pH 2.8) into 1/10th volume of 1 M Tris (pH 8.0). The column was washed with 0.5 M NaOH with a

minimum contact time of 15 min between purifications of different antibodies.

Coronavirus RBDs (SARS-CoV-2, SARS1, and MERS) were purified using HisPur Ni-NTA affinity resin (Thermo). Supernatants were diluted 1:1 with 10 mM imidazole/1× PBS and incubated with Ni-NTA resin for at least 1 h at 4°C while stirring. Resin/supernatant mixtures were then added to glass chromatography columns, washed with ~10 column volumes 10 mM imidazole/1× PBS, and RBDs were eluted using 250 mM imidazole / 1X PBS. Elutions were concentrated using Amicon spin filters (MWCO 10 kDa; Millipore Sigma) and RBDs were subsequently loaded onto a GE Superdex S200 increase 10/300 GL column pre-equilibrated in 1X PBS on a GE ÄKTA Pure system. Protein-containing fractions were identified by A280 signal and/or SDS-PAGE, pooled, and stored at 4°C or at −20°C in 10% glycerol/1× PBS until use.

2.4 | Isolation of fab from IgG

Lys-C endopeptidase (Wako) was added at a final concentration of 4 µg/ml to purified IgG (2 mg/ml in PBS + 100 mM Tris–HCl [pH 8.0]). This mixture was incubated for 1–1.5 h at 37°C with gentle shaking, then buffer exchanged to 50 mM NaOAc (pH 5.0) with Amicon spin filters (MWCO 10 kDa; Millipore Sigma). Fab was separated from undigested IgG and free Fc via cation exchange chromatography using a HiTrap SP HP column (Cytiva) over a 0–400 mM NaCl gradient in 50 mM NaOAc (pH 5.0). Purified Fab was buffer exchanged into 1× PBS (pH 7.4) for use in BLI.

2.5 | ACE2-huFc-Avi biotinylation

Purified ACE2 expressed with a human IgG1 Fc domain and C-terminal Avi tag was site-specifically biotinylated using BirA-thioredoxin. BirA enzyme was expressed and purified as previously described.[26] Briefly, BirA was expressed recombinantly in *Escherichia coli* as a genetic fusion to thioredoxin and purified with HisPur Ni-NTA affinity resin (Thermo Fisher Scientific). BirA-thioredoxin was subsequently loaded onto a GE Superdex S200 increase 10/300 GL column pre-equilibrated in 1× PBS on a GE ÄKTA Pure system before being aliquoted and frozen with 10% glycerol.

To biotinylate purified ACE2, briefly, ACE2 was buffered with 50 mM bicine (pH 8.3), 50 mM biotin, and 10 mM ATP. BirA enzyme was added at a ratio of 1:200 wt/wt and incubated for 1 h at 37°C before being buffer exchanged into PBS (pH 7.4) with a Zeba 7 kDa MWCO spin column (Thermo Fisher Scientific).

2.6 | Enzyme-linked immunosorbent assay

Nunc 96-well Maxisorp plates (Thermo) were coated with 50 µl of a 2 µg/ml RBD solution from SARS-CoV-1, SARS-CoV-2, or MERS-CoV in 50 mM sodium bicarbonate (pH 8.75) at room temperature for 1 h. Plates were then washed three times with MilliQ ddH$_2$O using an ELx 405 BioTek plate washer and blocked with 300 µl of Chonblock Blocking Buffer (Chondrex) at 4°C overnight. Chonblock was manually removed from plates and plates were subsequently washed three times with PBST (1× PBS [pH 7.4]/0.1% Tween-20). IgGs were diluted in PBST starting at 15 µg/ml with a five-fold dilution series. Antibody dilutions were added to each well and incubated at room temperature for 1 h. Plates were washed three times with PBST and then incubated with a goat anti-human HRP (abcam ab7153) secondary, at a 1:10000 dilution in PBST for 1 h at room temperature. Following secondary incubation, plates were washed six times with PBST and developed by adding 50 µl of 1-Step™ Turbo-TMB-ELISA Substrate Solution (Thermo Fisher Scientific 34,022) per well. Plates were quenched by adding 50 µl of 2 M H$_2$SO$_4$ per well and absorbance at 450 nm was quantified and normalized for path length using a BioTek Synergy HT Microplate Reader. Appropriate personal protective equipment (PPE) was used when working with acid and ELISA waste.

2.7 | BLI

His-tagged SARS-CoV-2 RBD (300 nM) was loaded on His1K biosensors (Pall ForteBio) to a load threshold of 0.4–0.6 nm except for scFv binding experiments in which biotinylated SARS-CoV-2 RBD was loaded on Streptavidin biosensors (Pall ForteBio). After a baseline step in assay buffer (PBS [pH 7.4], 0.1% bovine serum albumin, 0.05% Tween 20), ligand-loaded sensors were dipped into known concentrations of antibody for an association step and returned to the baseline well for dissociation. All samples in all experiments were baseline-subtracted to a well that loaded the tip with antibody, but did not go into sample, as a control for any buffer trends within the samples. Binding curves were fit using the "association then dissociation" equation in GraphPad Prism 8.4.1 to calculate K$_D$.

For ACE2 binding competition, experiments were performed in one of two ways. (1) Biotinylated ACE2 (300 nM) was loaded on Streptavidin biosensors (Pall ForteBio) to a load threshold of 0.4–0.6 nm. After a baseline step in assay buffer, ACE2-coated biosensors were dipped in a 300 nM solution of RBD for 5 min

before being dipped in a 100 nM solution of a given antibody. These results are reported in Figure 1(D). (2) RBD (300 nM) was loaded on His1K biosensors (Pall ForteBio) to a load threshold of 0.4–0.6 nm. After a baseline step in assay buffer, RBD-coated biosensors were dipped in a 300 nM solution of ACE2 or assay buffer for 5 min before being dipped in a 100 nM

solution of a given antibody. These results are reported in Figure S1E.

For antibody binding competition assays, His-tagged SARS-CoV-2 RBD (300 nM) was loaded on His1K biosensors (Pall ForteBio) to a load threshold of 0.4–0.6 nm. After a baseline step in assay buffer, RBD-coated biosensors were dipped in a 500 nM solution of a particular
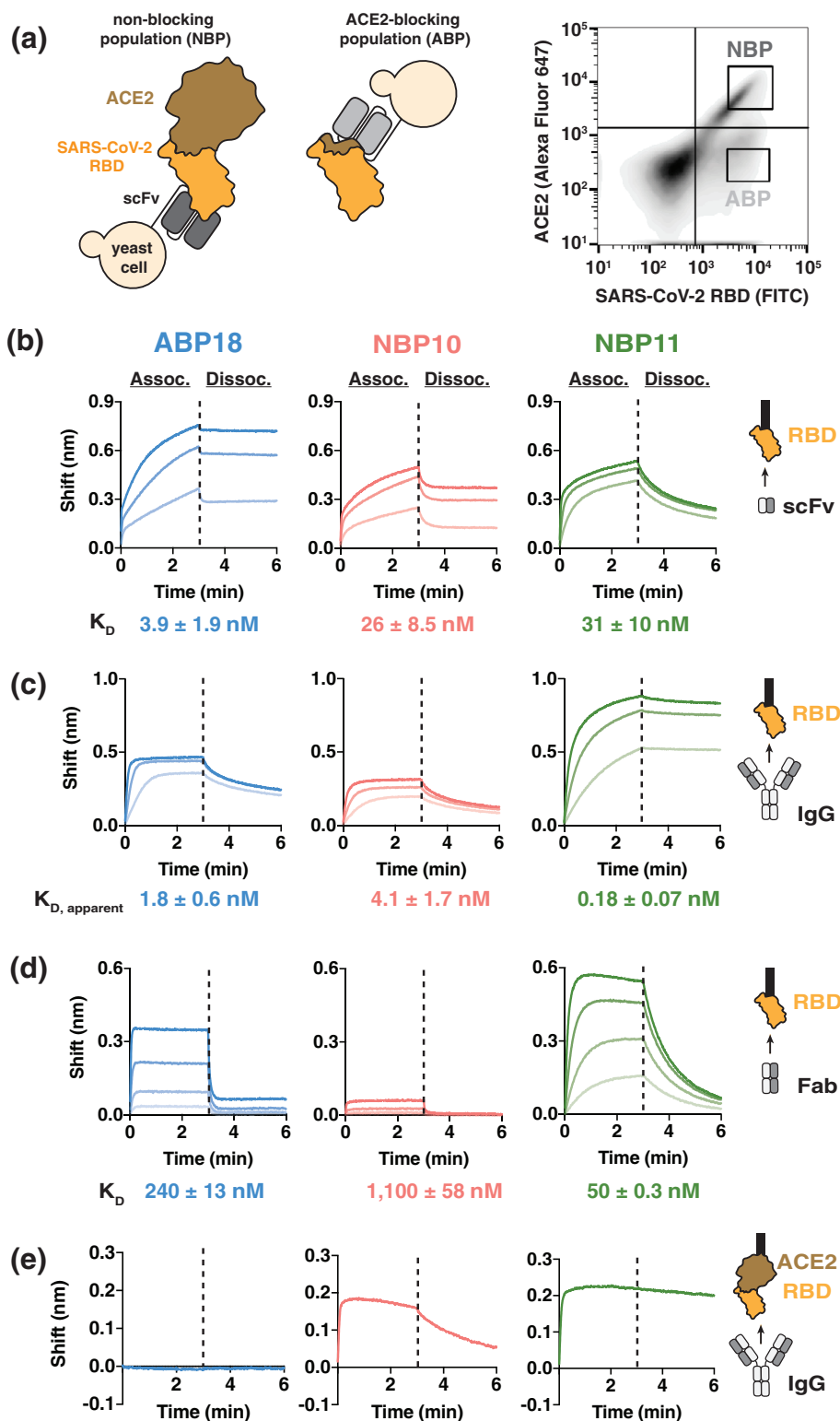

FIGURE 1 A human naïve antibody library yields antibodies targeting the SARS-CoV-2 receptor binding domain (RBD). (a) Left, selection scheme to isolate an ACE2-blocking population (ABP) and a non-blocking population (NBP) of antibodies. Right, flow cytometry panel of yeast display library with gates used to isolate the ABP and NBP. (b-d) Binding to SARS-CoV-2 RBD-coated BLI biosensors show substantial differences between (b) scFv antibody fragments (1,000, 333.3, and 111.1 nM), (c) IgG antibodies (100, 33.3, and 11.1 nM) and (d) Fab antibody fragments (ABP18/NBP11: 500, 167, 56, 18 nM; NBP10: 720, 240, 80, 27 nM). Higher antibody concentrations are indicated with thicker lines. (e) Binding of 100 nM IgG antibodies to BLI biosensors coated with ACE2:RBD complex shows that NBP10 and NBP11 IgG retain binding while ABP18 shows no binding, consistent with ACE2-blocking activity

"loaded" antibody for 4 min. "Loaded"-antibody/RBD-coated biosensors were then dipped in a 200 nM solution of a particular "associating" antibody for 3 min. The detected shift in nanometers of the "associating" antibody at 3 min in the absence of any "loaded" antibody was used as the maximal binding value. Values for the "loaded" antibody are reported as a fraction of this value. All BLI data were baseline-subtracted based on RBD-coated biosensors dipped into buffer for the "loading" and "associating" steps.

2.8 | Production of SARS-COV-2 pseudotyped lentivirus and viral neutralization assays

SARS-CoV-2 spike-pseudotyped lentivirus was produced as described.[20] Briefly, 6×10^6 HEK293T cells cultured in D10 medium (DMEM, 10% fetal bovine serum (Gemini Bio-Products), 2 mM L-glutamine, 1% penicillin/streptomycin, and 10 mM HEPES [pH 7.0]) were transfected at ~50–70% confluency using calcium phosphate transfection[20] with 5 lentiviral production plasmids: pHAGE_Luc packaging vector (10 μg), full-length SARS-CoV-2 spike (3.4 μg), HDM-Hgpm2 (2.2 μg), PRC-CMV-Rev1b (2.2 μg), and HDM-tat1b (2.2 μg).[27] Filter-sterilized plasmids were added to 0.5 ml sterile water followed by addition of 0.5 ml 2× HEPES-buffered saline (pH 7.0) (Alfa Aesar) and then dropwise addition of 100 μl 2.5 M $CaCl_2$. Transfections were incubated at room temperature for 20 min and then added dropwise to plated cells. Medium was exchanged ~18–24 h post transfection. Virus was harvested ~72 h post transfection via centrifugation at 300 x g for 5 min followed by filtration through a 0.45 μm filter. Viruses were aliquoted and stored at −80°C.

Neutralization assays were performed as described.[19,20] HeLa cells overexpressing ACE2[19] were plated at 5000 cells per well in clear-bottom white-walled 96-well plates 1 day prior to infection in D10 medium. Purified monoclonal antibodies were filtered using a 0.22 μm filter and then diluted using D10 medium. Virus was diluted in D10 medium and supplemented with polybrene (5 μg/ml final), added to inhibitor dilutions, and inhibitor/virus were incubated at 37°C for 1 h. Medium was removed from HeLa/ACE2 cells and replaced with virus/inhibitor mixtures which were then incubated for 48 h at 37°C. Cells were lysed via addition of BriteLite (Perkin Elmer) and luminescence signal from wells was determined using a BioTek plate reader.

Data from neutralization assays were processed using GraphPad Prism 8.4.1. Relative luminescence units from virus-only wells and cells-only wells were averaged, and RLU values from inhibitor neutralization curves were normalized to these averages (100% infection for virus only and 0% infection for cells only). Normalized infectivity values were then plotted as a function of inhibitor concentration and fit with a non-linear 3-parameter inhibitor curve to obtain IC_{50} values.

Appropriate personal protective equipment (lab coat and gloves) was used during including viral production and neutralization assays. All tissue culture work was performed in an approved and inspected biosafety cabinet.

3 | RESULTS

3.1 | A human naïve antibody library yields antibodies targeting the SARS-CoV-2 RBD

To isolate antibodies targeting the SARS-CoV-2 RBD, we panned the xEmplar™ yeast surface-display library (Materials and Methods); the xEmplar™ library is a naïve single-chain variable fragment (scFv) antibody library developed by xCella Biosciences with an estimated diversity of $\sim 1 \times 10^9$. This library is antigen-naïve, unrelated to SARS-CoV-2 infection, and has been used to identify antibodies against novel targets such as the immune checkpoint VISTA.[28]

We performed a total of five rounds of selection that included both magnetic- and fluorescence-activated cell sorting to enrich for RBD-binding clones (Materials and Methods [Section 2]). In the final round, we also used biotinylated ACE2 labeled with Streptavidin-Alexa Fluor 647 to differentiate between scFvs that disrupted the ACE2/RBD interaction (ACE2-blocking population) and those that did not (non-blocking population; Figure 1(a)). We identified a single unique sequence from the ACE2-blocking population (scFv ABP18) and three unique sequences from the non-blocking population (scFvs NBP10, NBP11, and NBP18); only ABP18, NBP10, and NBP11 were confirmed to bind RBD, both on the surface of yeast (Figure S1A) and when expressed recombinantly and tested by BLI (Figure 1(b)).

We cloned the variable heavy chain and variable light chain sequences into human IgG1 plasmids (Materials and Methods Section 2) to further characterize ABP18, NBP10, and NBP11. We used BLI to confirm binding to RBD and to determine whether these antibodies compete with ACE2, as expected based on the sorting scheme. RBD-coated biosensors bound ABP18, NBP10, and NBP11 in IgG form (Figure 1(c)), with low-nanomolar affinities calculated with a standard 1:1 binding model to simplify the bivalent interaction (Materials and Methods Section 2). To evaluate monovalent binding affinities, we

processed the IgGs to Fab fragments using the endoprotease Lys-C (Figure S1B). ABP18, NBP10, and NBP11 Fabs bound RBD (Figure 1(d)) and exhibited substantially faster dissociation rates than the IgG forms (compare Figure 1(c), (d)), suggesting that the slow off-rates for IgG/RBD binding were influenced by the avidity of the antibody binding site. We also observed a pronounced reduction in RBD affinity between scFv and Fab formats for ABP18 and NBP10 (Figure 1(b), (d)), as has been reported when altering the format of selected antibodies previously.[29–31] Consistent with the sequence and structural diversity among coronavirus RBDs,[32] enzyme-linked immunosorbent assays indicated that ABP18, NBP10, and NBP11 minimally bind RBDs from SARS-CoV-1 and MERS-CoV (Figure S1C).

To confirm that our selection scheme differentiated between ACE2-blocking and non-blocking scFv clones, we employed BLI in two orientations to assess the ability of these antibodies to interact with RBD in the presence of ACE2 (Figure S1D, S1E). When ACE2-coated biosensors were subsequently loaded with RBD, ABP18 showed

no binding (Figure 1(e)), while NBP10 and NBP11 IgG retained binding (Figure 1(e)). In the reverse binding orientation using RBD-coated biosensors loaded with ACE2, ABP18 IgG binding was reduced when biosensors were preloaded with ACE2 (Figure S1E); however, NBP10 and NBP11 IgG binding to RBD was unaffected by ACE2 (Figure S1E), validating the ability of our selection scheme to distinguish between ACE2-blocking and non-blocking antibodies.

3.2 | RBD antibodies neutralize SARS-CoV-2 spike-pseudotyped lentivirus

Not all RBD-targeting antibodies neutralize SARS-CoV-2 infection[10,33–35]; further, antibodies isolated against the RBD alone may not effectively target the RBD in the context of the full-length spike trimer. We therefore tested the ability of ABP18, NBP10, and NBP11 IgG to neutralize SARS-CoV-2 pseudotyped lentivirus infection of ACE2-expressing HeLa cells[19,27] (Figure 2(a)). All three

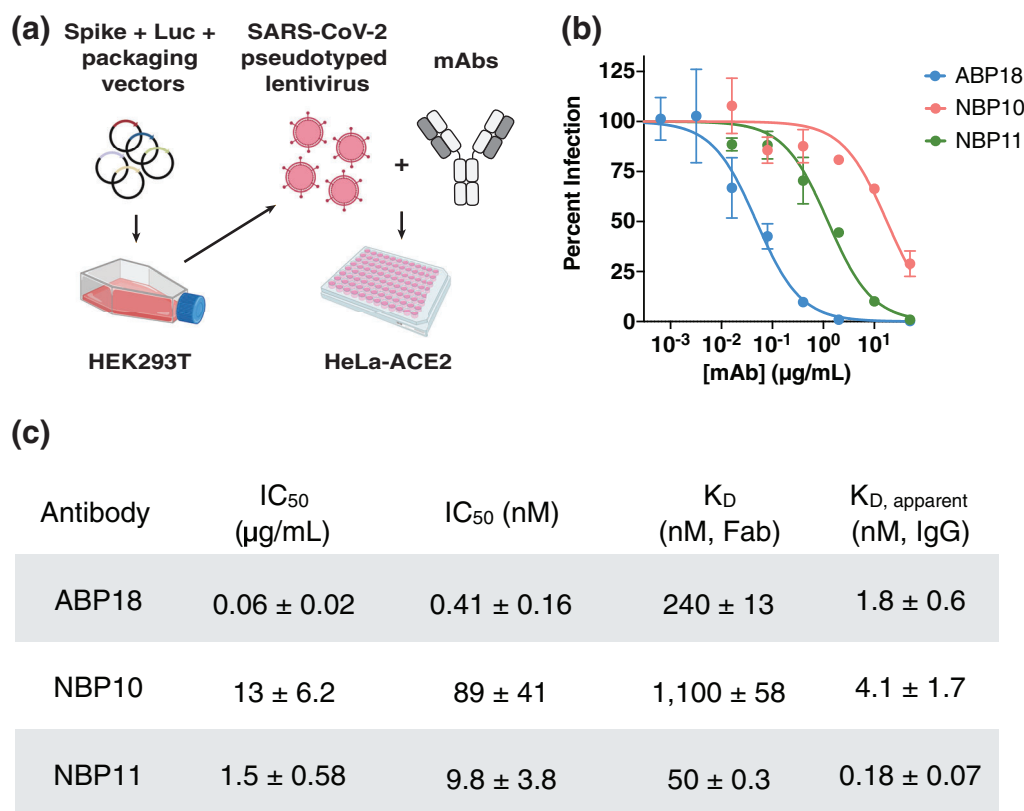| Antibody	IC_{50} (µg/mL)	IC_{50} (nM)	K_D (nM, Fab)	$K_{D, apparent}$ (nM, IgG)
ABP18	0.06 ± 0.02	0.41 ± 0.16	240 ± 13	1.8 ± 0.6
NBP10	13 ± 6.2	89 ± 41	1,100 ± 58	4.1 ± 1.7
NBP11	1.5 ± 0.58	9.8 ± 3.8	50 ± 0.3	0.18 ± 0.07

FIGURE 2 Receptor binding domain (RBD) antibodies neutralize SARS-CoV-2 spike-pseudotyped lentivirus. (a) SARS-CoV-2 spike-pseudotyped lentivirus produced in HEK293T cells encode firefly luciferase (Luc) and can infect HeLa cells stably expressing the ACE2 receptor (HeLa-ACE2).[19,20] Half maximal inhibitory concentration (IC_{50}) can be determined by titrating a monoclonal antibody (mAb) of interest. Figure created with BioRender.com. (b,c) ABP18, NBP10, and NBP11 IgG (b) neutralize SARS-CoV-2 spike-pseudotyped lentivirus in vitro with (c) IC_{50} values (mean ± SD) consistent with their true or apparent affinities. Representative inhibition curves are shown from repeated (n = 3) experiments

antibodies inhibited SARS-CoV-2 infection, with IC_{50} values ranging from 0.06 to 13 μg/ml (Figure 2(b), (c)).

ABP18 IgG had an IC_{50} value of 0.41 nM (Figure 2(c)), similar to its apparent affinity of 1.8 nM (Figure 2(c)), while NBP10 and NBP11 IgG had IC_{50} values ~20- to 50-fold weaker than their apparent affinities (Figure 2(c)). This difference may arise from (i) distinct mechanisms of viral neutralization employed by ABP18 and NBP10/NBP11 or (ii) differential epitope accessibility in the context of full-length spike or up/down conformations of the RBD.[10,36] Notably, all three antibodies have more potent IC_{50} values than their Fab binding affinities (Figure 2(c)), suggesting that antibody avidity plays an important role in viral neutralization.

3.3 | Neutralizing RBD antibodies have distinct but overlapping epitopes with antibodies elicited by natural COVID-19 infection

Several classes of RBD antibodies have been described based on binding competition experiments and structure determination.[6,10,13,19,33–35,37,38] We therefore sought to map the epitopes of ABP18, NBP10, and NBP11 using a BLI-based binding competition assay. We expressed and purified (Materials and Methods Section 2) a panel of nine published RBD antibodies elicited by natural COVID-19 infection, four of which (CB6,[38] P2B-2F6,[6] EY6A,[37] CR3022[33]) have high-resolution co-crystal structures available. Five antibodies were included from Brouwer et al.,[34] four of which (COVA1-12, COVA2-04, COVA2-07, COVA2-15) have low-resolution negative-stain electron-micrograph reconstructions available.[34] We included the fifth antibody from Brouwer et al.,[34] COVA2-05, because it represents a unique epitope class (compared to COVA1-12, COVA2-04, COVA2-07, and COVA2-15) and shares the same antibody heavy chain germline as NBP10 and NBP11 (Table S1). However, no structure is available for COVA2-05. This nine-antibody panel represents a range of RBD epitopes and antibody sequences, generated in vivo via patient responses to infection, by which to compare the antibodies that we isolated in vitro here.

To evaluate how ABP18, NBP10, and NBP11 compete with antibodies in this panel for binding to RBD, we used BLI to establish a binding competition matrix (Materials and Methods). RBD-coated biosensors were bound to saturation by an antibody (the "loaded" antibody). These loaded-antibody/RBD-coated biosensors were then bound to antibodies in solution (the "associating" antibody). The binding of an associating antibody to biosensors coated with RBD and loaded with a competing antibody

was compared to biosensors only coated with RBD and is reported as a fraction of maximal binding (Figure 3(a), S2A). Several ACE2-blocking antibodies (COVA1-12, COVA2-7, COVA2-4) displayed essentially the same competition binding profile (Figure S2A), motivating us to use a reduced panel to analyze the binding profiles of ABP18, NBP10, and NBP11 (Figure 3(b)).

NBP10 and NBP11 showed an identical pattern of binding competition (Figure 3(b)), suggesting that they share similar epitopes, consistent with their common heavy chain germline, IGHV5-51 (Table S1). NBP10 and NBP11 competed with COVA2-05, but not CR3022 or EY6A (Figure 3(b)). Interestingly, although EY6A and CR3022 have very similar epitopes,[37] COVA2-05 competed with CR3022, but not EY6A (Figure 3(b)). We therefore conclude that NBP10, NBP11, COVA2-05, CR3022, and EY6A share overlapping but distinct epitopes. One notable difference between the epitopes of CR3022 and EY6A is that the complementarity determining region loop 1 of the CR3022 light chain extends beyond the EY6A light chain footprint (Figure 3(a)), suggesting that this loop may be responsible for steric clashes between EY6A and NBP10/11. Combining our binding competition data and published structural data (Figure 3(c)), we determined putative footprints for NBP10, NBP11, and COVA2-05 (Figure 3(d)).

ABP18 demonstrated substantial competition with ACE2-blocking antibodies COVA1-12, COVA2-04, COVA2-07 (Figure S2B), and CB6 (Figure 3(b)), as expected. However, ABP18 did not compete with COVA2-15 or P2B-2F6 (Figure 3(b)), which are other ACE2-competing antibodies. Based on the high-resolution X-ray crystal structure of P2B-2F6[6] and the low-resolution negative-stain electron-micrograph reconstruction of COVA2-15,[34] we determined an approximate antibody footprint for ABP18 (Figure 3(e)). Although the RBD makes up a small region of the spike trimer, these antibody competition results confirmed previous reports[7,10,35] that the RBD contains several unique epitopes targeted by monoclonal antibodies. Further, the varied footprints and competition patterns even within the set of ACE2-competing antibodies tested here indicates that there are likely varied mechanisms of viral neutralization mediated by ACE2-blocking monoclonal antibodies.

4 | DISCUSSION

Understanding the humoral responses to SARS-CoV-2 infection and vaccination is critical to efforts aimed at curtailing the COVID-19 pandemic and establishing
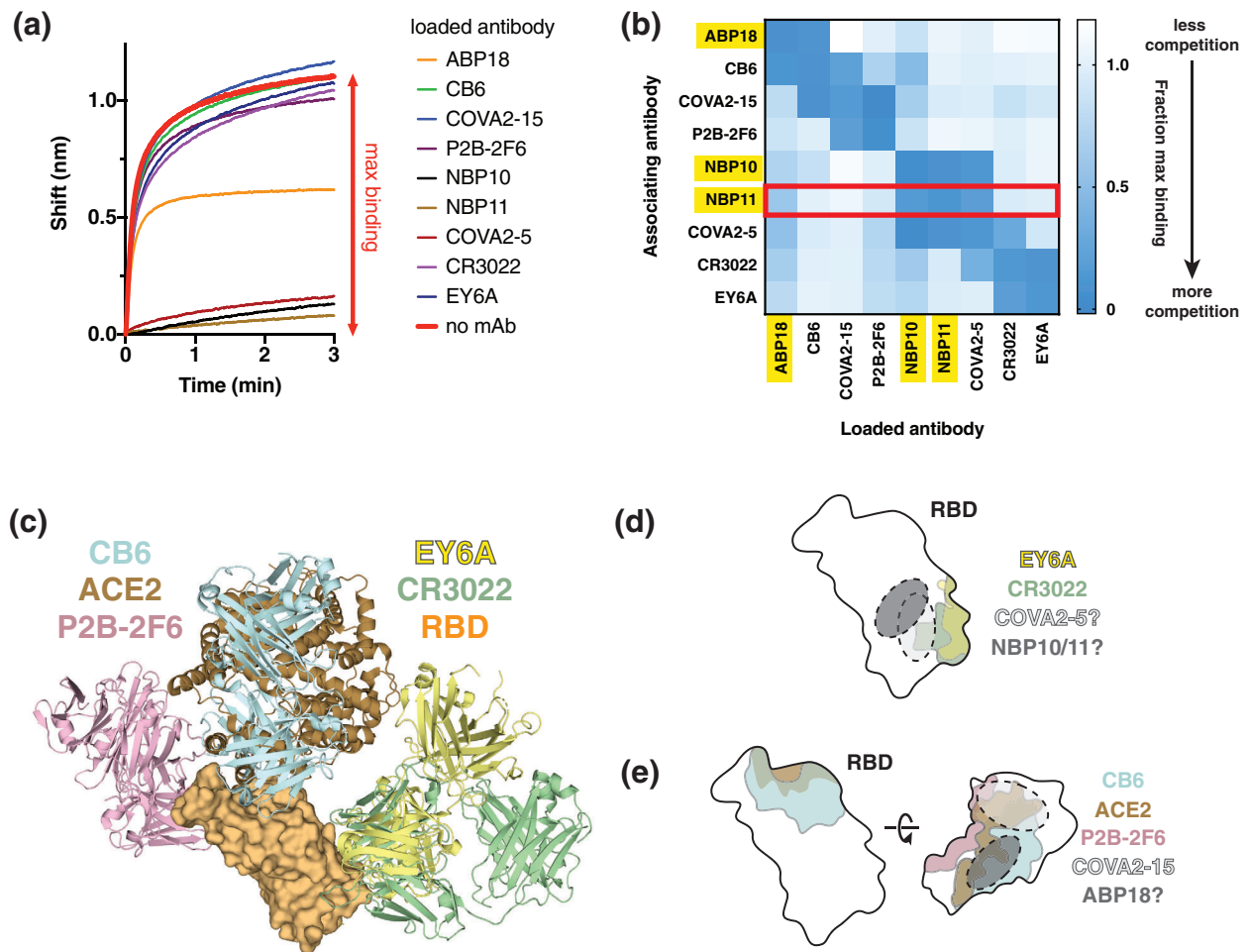
FIGURE 3 Neutralizing RBD antibodies have distinct but overlapping epitopes with antibodies elicited by natural COVID-19 infection. (a) Representative data from a biolayer interferometry (BLI)-based antibody competition assay with NBP11. RBD-coated biosensors were bound to saturation with an antibody ("loaded antibody") before being dipped in a solution of NBP11 IgG ("associating antibody"). The shift observed when binding RBD-coated biosensors loaded with no antibody (red) is used to calculated fractional maximal binding. (b) Antibody competition matrix determined by BLI identifies approximate epitopes of ABP18, NBP10, and NBP11. Fractional maximal binding values for loaded antibodies (x-axis) dipped into solutions of associating antibodies (y-axis) are shown. Converted data for NBP11 in panel A are boxed in red. (c) Reported co-crystal structures of antibodies P2B-2F6 (PBD: 7BWJ), CB6 (7C01), CR3022 (6W41), EY6A (6ZER) against the RBD used for epitope mapping experiments; ACE2 (6M17) is shown for reference. (d,e) Approximate epitopes of (d) NBP10/11 and (e) ABP18 based on published binding data and X-ray crystal structures of indicated antibodies.[6,33,37,38] The approximate footprint of COVA2-15 is based on published negative-stain electron microscopy[34]

effective correlates of protection. Accordingly, numerous patient-derived antibodies have been described, many of which target the RBD and have high similarity to germline antibody precursors. To exploit this similarity and to expand the repertoire of neutralizing antibodies, here we applied in vitro selections of a yeast surface-display library of human naïve antibodies to isolate and characterize three novel neutralizing antibodies that target the RBD: ABP18, NBP10, and NBP11 (Figure 1).

These antibodies neutralized SARS-CoV-2 spike-pseudotyped lentivirus in vitro (Figure 2), targeting the ACE2-binding site (ABP18) and other RBD

epitopes (NBP10 and NBP11) (Figure 3). BLI-based epitope mapping experiments revealed that the epitopes of these novel antibodies are distinct but overlapping with antibodies elicited by natural COVID-19 infection (Figure 3(b)). This work demonstrates that in vitro selections of naïve antibody repertoires can effectively mimic the antibody response in vivo in response to SARS-CoV-2 infection or vaccination, showcasing the value of this approach in rapidly isolating novel antibodies with therapeutic potential.

Blocking the ACE2:RBD interaction is a well-documented mechanism of action for neutralizing SARS-CoV-2 antibodies and is consistent with the binding

profile of ABP18. The mechanism by which NBP10 and NBP11 neutralize SARS-CoV-2 is unclear. It is possible that they bind outside the ACE2 binding site and prevent the RBD from sampling the up conformation.[10,36] This is the putative mechanism of EY6A, which neutralizes SARS-CoV-2, and CR3022, which neutralizes SARS-CoV-1.[37] Notably, NBP10 and NBP11 have overlapping epitopes with CR3022 (Figure 3(b), d)).

RBD-targeting antibodies bind numerous distinct, but overlapping, epitopes. We selected a panel of patient-derived RBD antibodies with well-defined epitopes and determined that none of them shared identical profiles with ABP18, NBP10, or NBP11 in binding competition experiments (Figure 3(b)). Each of our three novel antibodies demonstrated strong competition with at least one antibody in the binding panel, which in turn had strong competition with additional antibodies (Figure 3(b)), enabling us to delineate putative epitopes for ABP18, NBP10, and NBP11 (Figure 3(d),(e)). High-resolution structural information is needed to more precisely determine these antibody binding sites and their binding angles. Binding angles can be a critical factor in viral neutralization[39]; for example, antibodies such as CR3022 and EY6A complete strongly for binding the RBD, but only EY6A neutralizes SARS-CoV-2 entry.[37] Nevertheless, our results highlight how methods like BLI can quickly delineate classes of antibodies and provide low-resolution structural parameters for antibody:antigen interactions.

Antibodies with high similarity to the germline, and from diverse germline lineages, bind the RBD and can effectively neutralize SARS-CoV-2.[7,10,35] The antibodies described here also displayed high germline similarity, with low degrees of somatic hypermutation (Table S1). This observation is particularly promising for RBD- and spike-based vaccination strategies, as they may readily elicit neutralizing antibodies in patients presenting varied human antibody repertoires. There is well-documented enrichment of specific antibody germlines among antibodies elicited by SARS-CoV-2 infection, including IGHV1-24, IGVH1-69, IGHV3-30, IGHV3-53, and IGHV5-51.[7,8,34,40] The antibodies that we isolated here have sequences derived from these major germlines elicited in COVID-19 patients (Table S1). ABP18 is an IGHV1-69 antibody, a common germline regularly elicited by influenza infection[41] and enriched among SARS-CoV-2 antibodies.[34] By contrast, NBP10 and NBP11 both utilize IGHV5-51, consistent with their shared epitope. NBP11 shares both heavy and light chain germlines (IGHV5-51 and IGKV1-5, respectively) with C110, a recently described neutralizing RBD antibody derived from a COVID-19 patient.[35] Interestingly, the epitope of P2B-2F6 overlaps with that of C110,[10] though P2B-2F6 does not compete with NBP11 (Figure 3(b)), suggesting that C110 and NBP11 target distinct epitopes. This result further illustrates the diversity of near-germline antibodies that can effectively target the RBD, and underscores that even antibodies with the same germline precursors can target distinct RBD epitopes.

Taken together, these analyses highlight how in vitro selections of naïve antibodies can mimic the humoral response in vivo to identify neutralizing antibodies against novel human pathogens like SARS-CoV-2. Additionally, these novel RBD-targeting antibodies demonstrate the numerous distinct epitopes that can be effectively targeted on the SARS-CoV-2 RBD, bolstering COVID-19 therapeutic and vaccine efforts.

AUTHOR CONTRIBUTIONS

Benjamin Bell: Investigation; resources; visualization; writing-original draft; writing-review and editing. **Abigail Powell:** Investigation; resources; writing-review and editing. **Carlos Rodriguez:** Investigation; resources; writing-review and editing. **Jennifer Cochran:** Supervision; writing-review and editing. **Peter Kim:** Supervision; writing-review and editing.

CONFLICT OF INTEREST

Carlos Rodriguez is a former employee of xCella Biosciences. Jennifer R. Cochran is a co-founder and equity holder of xCella Biosciences. The other authors declare no conflict of interest.

ORCID

Benjamin N. Bell https://orcid.org/0000-0001-5356-0173

Peter S. Kim https://orcid.org/0000-0001-6503-4541

REFERENCES

1. (2020) WHO Coronavirus Disease (COVID-19) Dashboard. https://covid19.who.int/.
2. Hoffmann M, Kleine-Weber H, Schroeder S, et al. SARS-CoV-2 cell entry depends on ACE2 and TMPRSS2 and is blocked by a clinically proven protease inhibitor. Cell. 2020; 181:271–280.
3. Andersen KG, Rambaut A, Lipkin WI, Holmes EC, Garry RF. The proximal origin of SARS-CoV-2. Nat Med. 2020;26: 450–452.
4. Anderson DE, Tan CW, Chia WN, et al. Lack of cross-neutralization by SARS patient sera towards SARS-CoV-2. Emerg Microbes Infect. 2020;9:900–902.
5. Lv H, Wu NC, Tsang OTY, et al. Cross-reactive antibody response between SARS-CoV-2 and SARS-CoV infections. Cell Rep. 2020;31:107725.
6. Ju B, Zhang Q, Ge J, et al. Human neutralizing antibodies elicited by SARS-CoV-2 infection. Nature. 2020;584:115–119.
7. Robbiani DF, Gaebler C, Muecksch F, et al. Convergent antibody responses to SARS-CoV-2 in convalescent individuals. Nature. 2020;584:437–442.
8. Nielsen SCA, Yang F, Jackson KJL, et al. Human B cell clonal expansion and convergent antibody responses to SARS-CoV-2. Cell Host Microbe. 2020;28:516–525.
9. Ni L, Ye F, Cheng ML, et al. Detection of SARS-CoV-2-specific humoral and cellular immunity in COVID-19 convalescent individuals. Immunity. 2020;52:971–977.
10. Barnes CO, West AP, Huey-Tubman KE, et al. Structures of human antibodies bound to SARS-CoV-2 spike reveal common epitopes and recurrent features of antibodies. Cell. 2020;182: 828–842.
11. Seydoux E, Homad LJ, MacCamy AJ, et al. Analysis of a SARS-CoV-2-infected individual reveals development of potent neutralizing antibodies with limited somatic mutation. Immunity. 2020;53:98–105.
12. Röltgen K, Powell AE, Wirz OF, et al. Defining the features and duration of antibody responses to SARS-CoV-2 infection associated with disease severity and outcome. Sci Immunol. 2020;5:eabe0240.
13. Cao Y, Su B, Guo X, et al. Potent neutralizing antibodies against SARS-CoV-2 identified by high-throughput single-cell sequencing of convalescent patients' B cells. Cell. 2020;182: 73–84.
14. Gao Q, Bao L, Mao H, et al. Development of an inactivated vaccine candidate for SARS-CoV-2. Science. 2020;369:77–81.
15. Ravichandran S, Coyle EM, Klenow L, et al. Antibody signature induced by SARS-CoV-2 spike protein immunogens in rabbits. Sci Trans Med. 2020;12:eabc3539.
16. van Doremalen N, Lambe T, Spencer A, et al. ChAdOx1 nCoV-19 vaccination prevents SARS-CoV-2 pneumonia in rhesus macaques. Nature. 2020;586:578–583.
17. Du L, Zhao G, Li L, et al. Antigenicity and immunogenicity of SARS-CoV S protein receptor-binding domain stably expressed in CHO cells. Biochem Biophys Res Commun. 2009;384: 486–490.
18. Quinlan BD, Mou H, Zhang L, et al. The SARS-CoV-2 receptor-binding domain elicits a potent neutralizing response without antibody-dependent enhancement. bioRxiv. 2020. https://doi.org/10.1101/2020.04.10.036418.
19. Rogers TF, Zhao F, Huang D, et al. Isolation of potent SARS-CoV-2 neutralizing antibodies and protection from disease in a small animal model. Science. 2020;369:956–963.
20. Powell AE, Zhang K, Sanyal M, et al. A single immunization with spike-functionalized ferritin vaccines elicits neutralizing antibody responses against SARS-CoV-2 in mice. ACS Cent Sci. 2021;7:183–199.
21. Premkumar AL, Segovia-Chumbez B, Jadi R, et al. The RBD of the spike protein of SARS-group coronaviruses is a highly specific target of SARS-CoV-2 antibodies but not other pathogenic human and animal coronavirus antibodies. medRxiv. https://doi.org/10.1101/2020.05.06.20093377.
22. Shang J, Wan Y, Luo C, et al. Cell entry mechanisms of SARS-CoV-2. Proc Natl Acad Sci U S A. 2020;117:11727–11734.
23. Wang Q, Zhang Y, Wu L, et al. Structural and functional basis of SARS-CoV-2 entry by using human ACE2. Cell. 2020;181:894–904.
24. Glanville J, Zhai W, Berka J, et al. Precise determination of the diversity of a combinatorial antibody library gives insight into the human immunoglobulin repertoire. Proc Natl Acad Sci U S A. 2009;106:20216–20221.
25. Amanat F, Stadlbauer D, Strohmeier S, et al. A serological assay to detect SARS-CoV-2 seroconversion in humans. Nat Med. 2020;26:1033–1036.
26. Li Y, Sousa R. Expression and purification of *E. coli* BirA biotin ligase for in vitro biotinylation. Protein Expr Purif. 2012;82: 162–167.
27. Crawford KH, Eguia R, Dingens AS, et al. Protocol and reagents for pseudotyping lentiviral particles with SARS-CoV-2 spike protein for neutralization assays. Viruses. 2020; 12:513.
28. Mehta N, Maddineni S, Kelly RL, et al. An engineered antibody binds a distinct epitope and is a potent inhibitor of murine and human VISTA. Sci Rep. 2020;10:15171.
29. Menzel C, Schirrmann T, Konthur Z, Jostock T, Dübel S. Human antibody RNase fusion protein targeting CD30+ lymphomas. Blood. 2008;111:3830–3837.
30. Steinwand M, Droste P, Frenzel A, Hust M, Dübel S, Schirrmann T. The influence of antibody fragment format on phage display based affinity maturation of IgG. mAbs. 2014;6: 204–218.
31. Thie H, Toleikis L, Li J, et al. Rise and fall of an anti-MUC1 specific antibody. PLoS One. 2011;6:e0015921.
32. Li F. Structure, function, and evolution of coronavirus spike proteins. Annu Rev Virol. 2016;3:237–261.
33. Yuan M, Wu NC, Zhu X, et al. A highly conserved cryptic epitope in the receptor binding domains of SARS-CoV-2 and SARS-CoV. Science. 2020;368:630–633.
34. Brouwer PJ, Caniels TG, van der Straten K, et al. Potent neutralizing antibodies from COVID-19 patients define multiple targets of vulnerability. Science. 2020;369:643–650.
35. Barnes CO, Jette CA, Abernathy ME, et al. SARS-CoV-2 neutralizing antibody structures inform therapeutic strategies. Nature. 2020;588:682–687.

36. Cai Y, Zhang J, Xiao T, et al. Distinct conformational states of SARS-CoV-2 spike protein. Science. 2020;369:1586–1592.

37. Zhou D, Duyvesteyn HME, Chen C-P, et al. Structural basis for the neutralization of SARS-CoV-2 by an antibody from a convalescent patient. Nat Struct Mol Biol. 2020;27:950–958.

38. Shi R, Shan C, Duan X, et al. A human neutralizing antibody targets the receptor-binding site of SARS-CoV-2. Nature. 2020; 584:120–124.

39. Murin CD, Wilson IA, Ward AB. Antibody responses to viral infections: A structural perspective across three different enveloped viruses. Nat Microbiol. 2019;4:734–747.

40. Zost SJ, Gilchuk P, Chen RE, et al. Rapid isolation and profiling of a diverse panel of human monoclonal antibodies targeting 3 the SARS-CoV-2 spike protein 4 5. Nat Med. 2020; 26:1422–1427.

41. Avnir Y, Watson CT, Glanville J, et al. IGHV1-69 polymorphism modulates anti-influenza antibody repertoires, correlates with IGHV utilization shifts and varies by ethnicity OPEN. Sci Rep. 2016;6:20842.

SUPPORTING INFORMATION

Additional supporting information may be found online in the Supporting Information section at the end of this article.